Supporting Information:

Construction of Laminated Luminescent Solar Concentrator "Smart" Window Based on Thermoresponsive Polymer and Carbon Quantum Dots

Bing Xu [1], Jianying Wang [1,*], Chen Cai [1], Wei Xin [1], Lai Wei [2,*], Qinsi Yang [3], Bo Peng [3], Yuandu Hu [4], Jinhua Li [1,*], Xianbao Wang [1]

[1] Key Laboratory for the Green Preparation and Application of Functional Materials, Ministry of Education, Collaborative Innovation Center for Advanced Organic Chemical Materials Co-constructed by the Province and Ministry, Hubei Key Laboratory of Polymer Materials, School of Materials Science and Engineering, Hubei University, Wuhan 430062, P. R. China.

[2] Wuhan Drug Solubilization and Delivery Technology Research Center, School of Life and Health, Wuhan Vocational College of Software and Engineering, Wuhan 430205, P. R. China.

[3] Wenzhou Institute, University of Chinese Academy of Sciences, Wenzhou, Zhejiang 325000, P. R. China.

[4] Department of Materials Science and Engineering, School of Physical Sciences and Engineering, Beijing Jiaotong University, Beijing 100044, P. R. China.

Characterization

To characterizing the morphology and diameter of the B/G-CQDs, the high-resolution field-emission transmission electron microscope (HRTEM) was conducted on Talos F200X (FEI, Czech). Fourier Transform infrared spectroscopy (FT-IR) was carried out on a NICOLET iS50 spectrophotometer (Thermo Fisher Scientific, America). The elemental analysis was obtained through X-ray photoelectron spectra (XPS) (PHOIBOS150, Germany). Photographs of all the LSCs under visible and UV light were monitored by a common camera. The UV-vis absorption spectra of B/G-CQDs were measured using UV-vis absorption spectrometer (UV-3600 Plus, Shimadzu, Japan). The PL excitation and emission spectra of B/G-CQDs were tested via the fluorescent spectrometer (RF-6000, Shimadzu, Japan). The steady-state photoluminescence (PL) and time resolved photoluminescence (TRPL) (under 420 nm excitation) was obtained by DW-PLE03 (Fluo Time 300). The current density-voltage (*J-V*) curves of the silicon solar cell were measured by a source meter (Keithley 2400, USA) under simulated AM 1.5 G (100 mW·cm^{-2} irradiance) provided by a solar simulator (Newport Oriel Sol 3A Class AAA, 64023A). Silicon solar cells (V_{oc}: 0.54 V, J_{sc}: 30 mA/cm^2, PCE:11% (active area: 0.5 cm^2), EQE:16%) is purchased from Ningbo Angui Electronics Co., Ltd. The PLQYs (η_{PL}) of all the LSCs were measured on fluorescence spectrophotometer (Ocean Optics QE65PRO-FL) with a calibrated integrating sphere. The external optical efficiency (η_{opt}) can be calculated by using the following equation: $\eta_{opt} = \frac{I_{LSC}}{I_{sc}*G}$, where I_{LSC} is the short circuit current from a cell attached to the LSC and I_{SC} is the short circuit current measured

for the same solar cell under direct illumination with the same light source. *G* is a ratio of the top surface area (A_{top}) relative to the edge surface area (A_{edge}) of the LSC. A majority of surface area of the silicon solar cell was covered by a black tape and the left surface area of the solar cell is strictly the same as one edge area of the LSCs for measurement of optical efficiency. The IPCE measurements were carried out on Newport TLS130B-300X measure system. The data were collected by illuminating the device under monochromatic light using a 300 W xenon lamp.

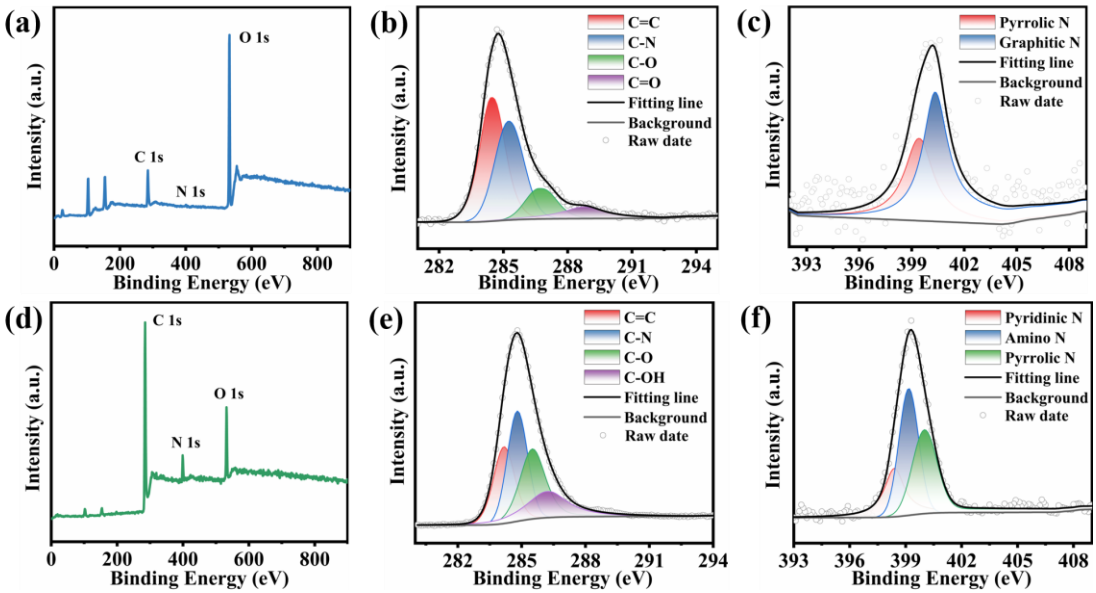

Figure S1. The high-resolution XPS spectra of (a) the full spectrum, (b) C 1s and (c) N 1s peaks of B-CQDs. The high-resolution XPS spectra of (d) the full spectrum, (e) C 1s and (f) N 1s peaks of G-CQDs.

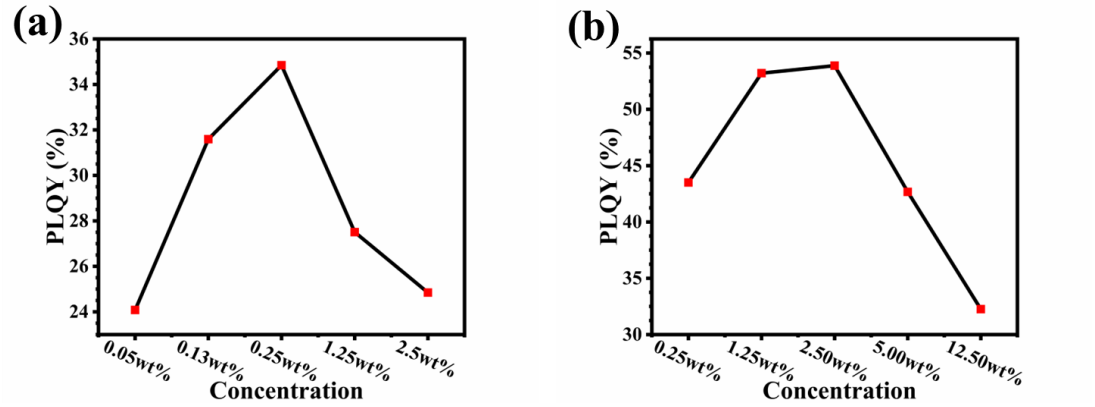

Figure S2. The PLQYs of (a) B-LSC-SW and (b) G-LSC-SW at different CQDs concentrations.

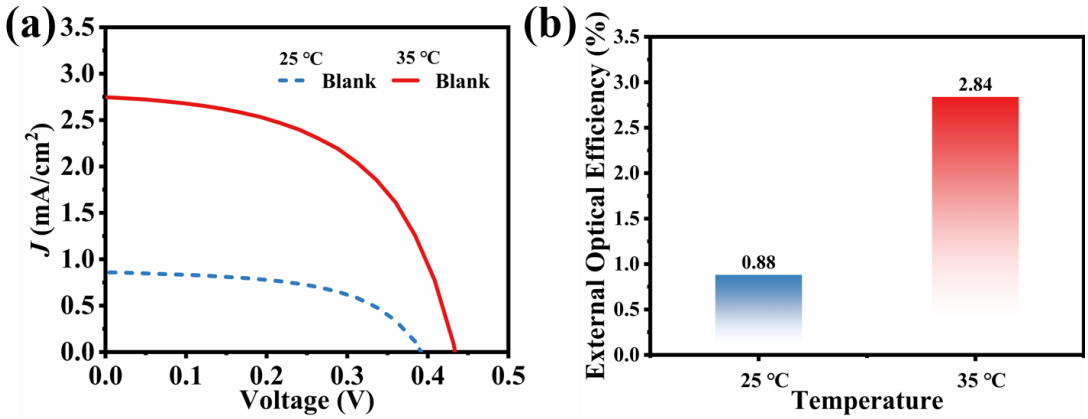

Figure S3. (a) *J-V* curve of the control LSC-SW (only containing thermoresponsive polymer without CQDs) at 25 °C and 35 °C. (b) External optical efficiencies of the control LSC-SW at 25 °C and 35 °C.

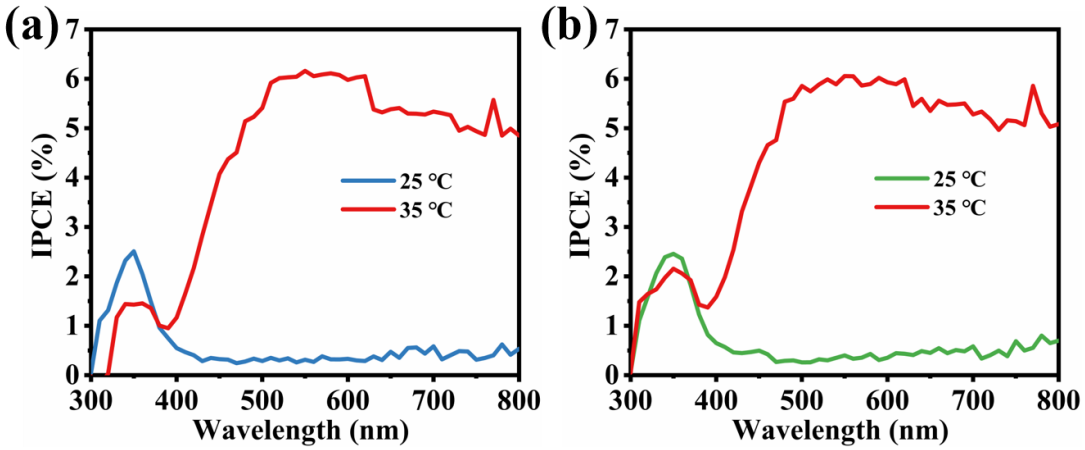

Figure S4. Incident photon-to-current conversion efficiency (IPCE) of (a) B-LSC-SW and (b) G-LSC-SW at 25 °C and 35 °C, respectively.

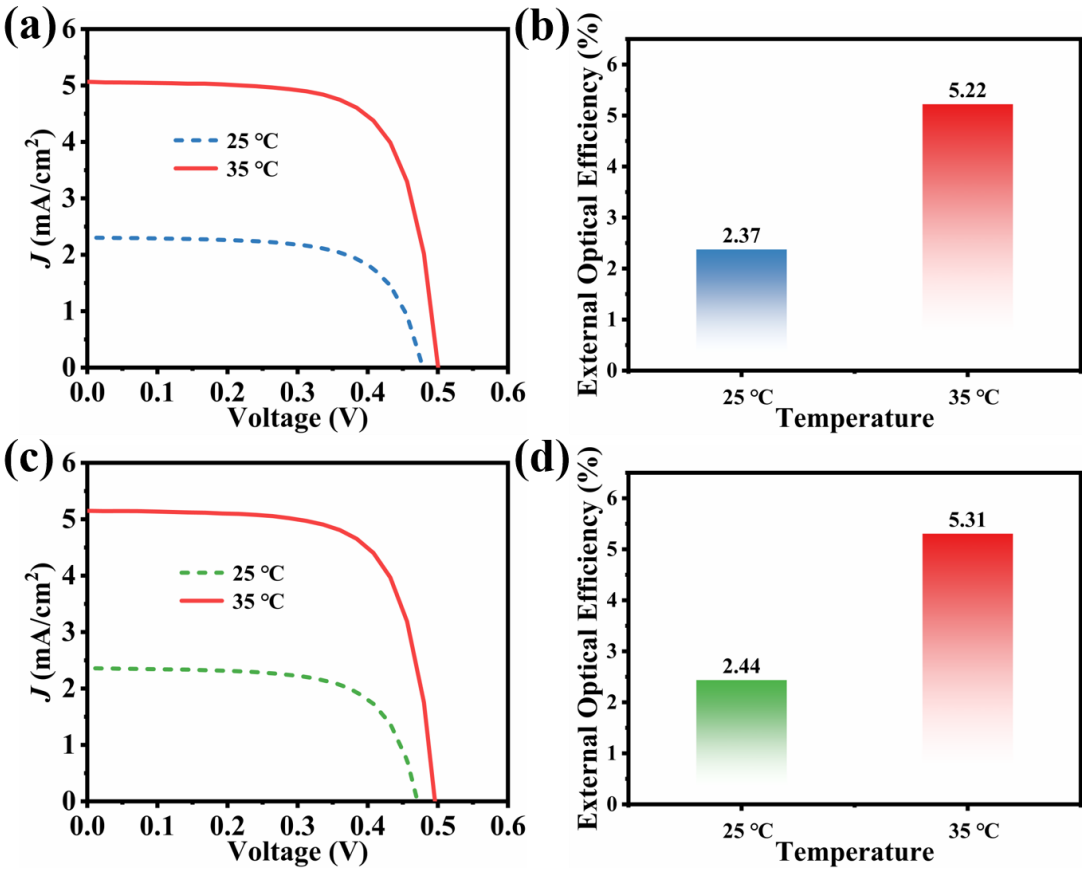

Figure S5. *J-V* curve of large area (5×5×0.2 cm^3) (a) B-LSC-SW (CQDs concentration at 0.25 wt%) and (c) G-LSC-SW (CQDs concentration at 2.5 wt%) at 25 °C and 35 °C, respectively. External optical efficiencies of large area (b) B-LSC-SW and (d) G-LSC-SW at 25 °C and 35 °C, respectively.

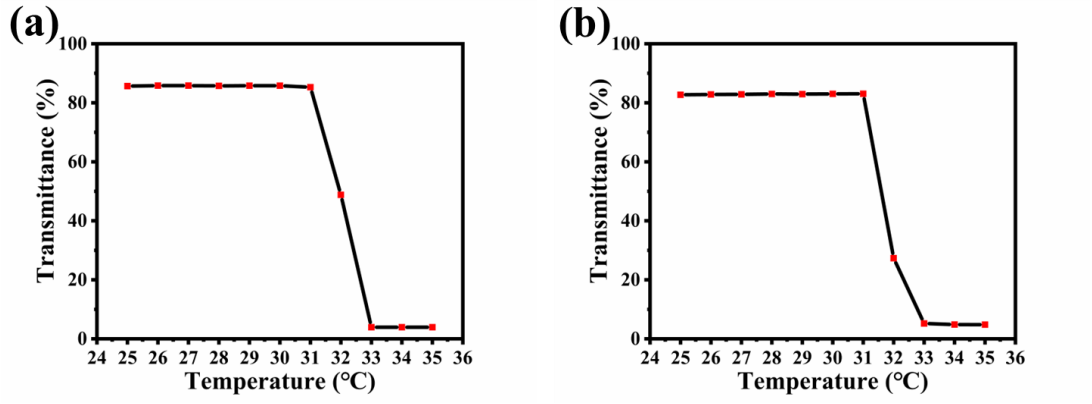

Figure S6. The transmittance of (a) B-LSC-SW at 0.25 wt% of B-CQDs and (b) G-LSC-SW at 2.50 wt% of G-CQDs at 650 nm under different ambient temperatures.

Table S1. Lifetime data and the PLQYs for B-CQDs and G-CQDs solutions (under 375 nm excitation).

	PLQY (%)	A_1	τ_1 (ns)	A_2	τ_2 (ns)	τ_{avg} (ns)	χ^2
B-CQDs	3.67	0.26	37.00	11.20	13.77	15.1	0.999
G-CQDs	13.26	0.31	20.10	7.71	8.89	9.8	0.999

Table S2. Photovoltaic parameters of B-LSC windows.

Temperature	$C_{B\text{-}CQDs}$	J_{LSC}/mA/cm^2	V_{OC}/V	*FF*	η_{opt} (%)
25 ℃	0.05 wt%	2.07	0.40	0.52	2.13
	0.13 wt%	2.38	0.41	0.54	2.45
	0.25 wt%	2.53	0.42	0.54	2.61
	1.25 wt%	2.37	0.42	0.54	2.45
	2.50 wt%	2.45	0.42	0.54	2.53
35 ℃	0.05 wt%	7.12	0.47	0.61	7.25
	0.13 wt%	7.11	0.47	0.62	7.35
	0.25 wt%	7.25	0.47	0.62	7.49
	1.25 wt%	7.01	0.47	0.62	7.23
	2.50 wt%	6.81	0.47	0.61	7.04

Table S3. Photovoltaic parameters of G-LSC windows.

Temperature	$C_{G\text{-}CQDs}$	J_{LSC} (mA/cm^2)	V_{OC} (V)	*FF*	η_{opt} (%)
25 ℃	0.25 wt%	2.04	0.41	0.53	2.10
	1.25 wt%	2.57	0.43	0.55	2.65
	2.50 wt%	2.67	0.41	0.50	2.76
	5.00 wt%	2.59	0.42	0.55	2.68
	12.50 wt%	2.21	0.42	0.54	2.28

	0.25 wt%	6.68	0.45	0.61	6.90
	1.25 wt%	6.83	0.47	0.62	7.05
35 ℃	2.50 wt%	6.97	0.47	0.62	7.20
	5.00 wt%	6.30	0.45	0.61	6.50
	12.50 wt%	5.69	0.46	0.60	5.87

Table S4. PLQYs of B-LSC windows.

$C_{\text{B-CQDs}}$	PLQY (%)
0.05 wt%	24.08
0.13 wt%	31.59
0.25 wt%	34.84
1.25 wt%	27.51
2.50 wt%	24.85

Table S5. PLQYs of G-LSC windows.

$C_{\text{G-CQDs}}$	PLQY (%)
0.25 wt%	43.50
1.25 wt%	53.21
2.50 wt%	53.88
5.00 wt%	42.67
12.50 wt%	32.25